J|A|C|S
ARTICLES

A Biomimetic Potassium Responsive Nanochannel: G-Quadruplex DNA Conformational Switching in a Synthetic Nanopore

Xu Hou,[‡] Wei Guo,[§] Fan Xia,[†] Fu-Qiang Nie,[†] Hua Dong,[†] Ye Tian,[†] Liping Wen,[†]
Lin Wang,[§] Liuxuan Cao,[§] Yang Yang,[‡] Jianming Xue,[§] Yanlin Song,[†]
Yugang Wang,*,[§] Dongsheng Liu,*,[‡] and Lei Jiang*,[†]

*Center of Molecular Sciences, Institute of Chemistry, Chinese Academy of Sciences,
Beijing 100190, People's Republic of China, National Center for Nanoscience and
Nanotechnology, Beijing 100190, People's Republic of China, and State Key Laboratory of
Nuclear Physics and Technology, Peking University, Beijing 100871, People's Republic of China*

Received February 28, 2009; E-mail: jianglei@iccas.ac.cn; ygwang@pku.edu.cn; liuds@nanoctr.cn

Abstract: Potassium is especially crucial in modulating the activity of muscles and nerves whose cells have specialized ion channels for transporting potassium. Normal body function extremely depends on the regulation of potassium concentrations inside the ion channels within a certain range. For life science, undoubtedly, it is significant and challenging to study and imitate these processes happening in living organisms with a convenient artificial system. Here we report a novel biomimetic nanochannel system which has an ion concentration effect that provides a nonlinear response to potassium ion at the concentration ranging from 0 to 1500 μM. This new phenomenon is caused by the G-quadruplex DNA conformational change with a positive correlation with ion concentration. In this work, G-quadruplex DNA was immobilized onto a synthetic nanopore, which undergoes a potassium-responsive conformational change and then induces the change in the effective pore size. The responsive ability of this system can be regulated by the stability of G-quadruplex structure through adjusting potassium concentration. The situation of the grafting G-quadruplex DNA on a single nanopore can closely imitate the in vivo condition because the G-rich telomere overhang is attached to the chromosome. Therefore, this artificial system could promote a potential to conveniently study biomolecule conformational change in confined space by the current measurement, which is significantly different from the nanopore sequencing. Moreover, such a system may also potentially spark further experimental and theoretical efforts to simulate the process of ion transport in living organisms and can be further generalized to other more complicated functional molecules for the exploitation of novel bioinspired intelligent nanopore machines.

Introduction

Inspired by the biological ion channel, a synthetic film with a single nanopore structure was prepared as described by Apel et al.[1] Unlike the fragile lipid-bilayer membrane in which most natural ion channels are embedded, this synthetic film is mechanically and chemically robust. Recently, Martin and Siwy et al.[2] reported DNA−nanotube artificial ion channel systems that helped us to better understand the role of an electromechanical gate that responds to the applied voltage, and they also developed the function of this system with DNA single-base mismatch selectivity; ten Elshof et al. reported using the nanometer-sized pores of membrane gates to achieve the surfactant-modulated switching of molecular transport;[3] Letant

et al. reported localized functionalization of single nanopores;[4] Bashir et al. developed solid-state nanopore channels with DNA selectivity.[5] Most recently, we reported gating of single synthetic nanopores by proton-driven DNA molecular motors.[6] Azzaroni and Ali et al. reported supramolecular bioconjugation in a single nanopore as a biosensor and the pH-tunable rectifying characteristics of the single conical nanopores.[7] Even though ion channels in living organisms have been studied by a mimic method using synthetic nanopores during the past several

---

[†] Institute of Chemistry, Chinese Academy of Sciences.
[‡] National Center for Nanoscience and Nanotechnology.
[§] State Key Laboratory of Nuclear Physics and Technology, Peking University.
(1) Apel, P. *Radiat. Meas.* **2001**, *34*, 559–566.
(2) (a) Harrell, C. C.; Kohli, P.; Siwy, Z.; Martin, C. R. *J. Am. Chem. Soc.* **2004**, *126*, 15646–15647. (b) Kohli, P.; Harrell, C. C.; Cao, Z. H.; Gasparac, R.; Tan, W. H.; Martin, C. R. *Science* **2004**, *305*, 984–986.

(3) Schmuhl, R.; van den Berg, A.; Blank, D. H. A.; ten Elshof, J. E. *Angew. Chem., Int. Ed.* **2006**, *45*, 3341–3345.
(4) Nilsson, J.; Lee, J. R. I.; Ratto, T. V.; Letant, S. E. *Adv. Mater.* **2006**, *18*, 427–431.
(5) Iqbal, S. M.; Akin, D.; Bashir, R. *Nat. Nanotechnol.* **2007**, *2*, 243–248.
(6) Xia, F.; Guo, W.; Mao, Y. D.; Hou, X.; Xue, J. M.; Xia, H. W.; Wang, L.; Song, Y. L.; Ji, H.; Qi, O. Y.; Wang, Y. G.; Jiang, L. *J. Am. Chem. Soc.* **2008**, *130*, 8345–8350.
(7) (a) Ali, M.; Yameen, B.; Neumann, R.; Ensinger, W.; Knoll, W.; Azzaroni, O. *J. Am. Chem. Soc.* **2008**, *130*, 16351–16357. (b) Yameen, B.; M., A.; Neumann, R.; Ensinger, W.; Knoll, W.; Azzaroni, O. *J. Am. Chem. Soc.* **2009**, *131*, 2070–2071. (c) Ali, M.; Ramirez, P.; Ma, F.; Neumann, R.; Ensinger, W. *ACS Nano* **2009**, *3*, 603–608.

decades, how to endow these synthetic nanopores with intelligence is still a challenging task.

In this work, we further extend the function of molecule–nanopore systems by using G-quadruplex (G4) DNA.[8] In this biomimetic nanochannel system (BNCS), there is an ion concentration effect, which is a very important phenomenon in a living body and other systems do not have. This system is also different from the previous systems[2a] that utilized the different chain length of no-responsive DNA oligomers, chemisorbed on the pore walls and surface of the membrane. According to the pH influences on the nanopore, our previous work on a pH-responsive i-motif DNA–nanopore system focused on the permeability ratios of the single nanopore between two different pH values. On the basis of our prior work,[6,9] the present work is much different because this novel biomimetic nanochannel system was responsive to potassium ion (K$^+$) within a certain concentration range and simulated these processes in a pH-neutral environment as in a natural organism.[10]

G-Quadruplexes are highly ordered DNA structures derived from G-rich sequences formed by tetrads of hydrogen-bonded guanine bases. Among the quadruplex-forming sequences, the human telomeric sequence d[AGGG(TTAGGG)$_3$] has attracted tremendous interest due to its importance at telomere maintenance and cell aging or death.[8f] Recently, there are many researches on the conformational change of this biomolecule[8b,d,11] and its applications on artificial ion channels[12] and biosensors.[13]

Here we selected the G-rich human telomere strand[8g,h,11b,14] due to the possibility of forming the intramolecular four-stranded quadruplex topologies, and this process is dependent on the alkali metal ion concentration. Upon considering the efficiency at stabilizing G4 DNA, K$^+$ is much more effective than other alkali metal ions in promoting the formation of the G4 structures, whereas lithium ion (Li$^+$) is ineffective in all cases.[8d,15] Therefore, these two ions mentioned above were selected as control to investigate the ion-responsive properties of the BNCS.

We prepared a single nanopore membrane with the well-developed ion track-etching technique.[16] The nanopore (see Supporting Information, Scheme S1) was embedded in a track-etched polyethylene terephthalate membrane (PET, Hostaphan RN12 Hoechst, 12 μm thick, with single ion track in the center). The track-etching technique allows control over the shape of the pores, and in this work, the etched single nanopore is cone-like. Diameter measurement of the single conical nanopore was conducted with a commonly used electrochemical method.[16a,c] Its large opening (base) is usually several hundred nanometers, and the narrow opening (tip) is ~20 nm. During the etching process, negatively charged carboxyl groups, which were attached to flexible polymer chains, were created on the pore surface. Then, the amino single-stranded G4 DNA was immobilized onto the inner wall of the nanopore by a two-step chemical reaction[6] (see Supporting Information, Scheme S2). After grafting G4 DNA on a conical nanopore wall, the DNA underwent a potassium-responsive conformational change between a random single-stranded structure (no K$^+$) and a four-stranded G4 structure (presence of K$^+$), as shown in Scheme 1a and b. This conformational conversion could well induce a change in the effective pore size of the nanopore and thus realized K$^+$-responsive ion transport properties of the BNCS.

The responsive ion transport properties of this nanopore–DNA system were evaluated by measuring the ionic current across the channel in an environment under neutral conditions. Ionic current measurements were carried out with a Keithley 6487 picoammeter (Keithley Instruments, Cleveland, OH) in a custom-designed electrolyte cell, and the sample membrane was mounted between the two halves of the cell (see Supporting Information, Scheme S3). Each half-cell was filled with 2 mL of the electrolyte solution of tris(hydroxymethyl)aminomethane hydrochloride (Tris-HCl) at pH 7.2 with fixation temperature at 23 °C. For each test, the measurements of the Li$^+$ transport properties of this BNCS were first done. Then, the measurements of the K$^+$-responsive ion transport properties were carried out. Details of circular dichroism (CD) spectroscopy measurements, nanopore preparation, DNA immobilization, and ionic current measurements are given in the Experimental Section.

Results and Discussion

The conformational change of G4 DNA was determined by CD spectroscopy measurements. Control experiments showed that Li$^+$ had no obvious CD signal within the measured range when the concentration of Li$^+$ increased from 0 to 10 mM (Figure 1a). As shown in Figure 1b, when the concentration of

(8) (a) Smargiasso, N.; Rosu, F.; Hsia, W.; Colson, P.; Baker, E. S.; Bowers, M. T.; De Pauw, E.; Gabelica, V. *J. Am. Chem. Soc.* **2008**, *130*, 10208–10216. (b) Monchaud, D.; Yang, P.; Lacroix, L.; Teulade-Fichou, M. P.; Mergny, J. L. *Angew. Chem., Int. Ed.* **2008**, *47*, 4858–4861. (c) Maizels, N. *Nat. Struct. Biol.* **2006**, *13*, 1055–1059. (d) Alberti, P.; Bourdoncle, A.; Sacca, B.; Lacroix, L.; Mergny, J. L. *Org. Biomol. Chem.* **2006**, *4*, 3383–3391. (e) Dittmer, W. U.; Reuter, A.; Simmel, F. C. *Angew. Chem., Int. Ed.* **2004**, *43*, 3550–3553. (f) Davis, J. T. *Angew. Chem., Int. Ed.* **2004**, *43*, 668–698. (g) Patel, D. J. *Nature* **2002**, *417*, 807–808. (h) Parkinson, G. N.; Lee, M. P. H.; Neidle, S. *Nature* **2002**, *417*, 876–880.

(9) (a) Xie, Y. B.; Wang, X. W.; Xue, J. M.; Jin, K.; Chen, L.; Wang, Y. G. *Appl. Phys. Lett.* **2008**, *93*, 163116. (b) Wang, S. T.; Liu, H. J.; Liu, D. S.; Ma, X. Y.; Fang, X. H.; Jiang, L. *Angew. Chem., Int. Ed.* **2007**, *46*, 3915–3917. (c) Liu, Q.; Wang, Y.; Guo, W.; Ji, H.; Xue, J.; Ouyang, Q. *Phys. Rev. E* **2007**, *75*, 051201. (d) Wang, X. W.; Xue, J. M.; Wang, L.; Guo, W.; Zhang, W. M.; Wang, Y. G.; Liu, Q.; Ji, H.; Ouyang, Q. Y. *J. Phys. D: Appl. Phys.* **2007**, *40*, 7077–7084. (e) Mao, Y. D.; Chang, S.; Yang, S. X.; Ouyang, Q.; Jiang, L. *Nat. Nanotechnol.* **2007**, *2*, 366–371. (f) Mao, Y. D.; Liu, D. S.; Wang, S. T.; Luo, S. N.; Wang, W. X.; Yang, Y. L.; Qi, Q. Y.; Lei, J. *Nucleic Acids Res.* **2007**, *35*, e33(1).

(10) Domene, C.; Klein, M. L.; Branduardi, D.; Gervasio, F. L.; Parrinello, M. *J. Am. Chem. Soc.* **2008**, *130*, 9474–9480.

(11) (a) Lane, A. N.; Chaires, J. B.; Gray, R. D.; Trent, J. O. *Nucleic Acids Res.* **2008**, *36*, 5482–5515. (b) Phan, A. T.; Kuryavyi, V.; Luu, K. N.; Patel, D. J. *Nucleic Acids Res.* **2007**, *35*, 6517–6525. (c) Zhao, Y.; Kan, Z. Y.; Zeng, Z. X.; Hao, Y. H.; Chen, H.; Tan, Z. *J. Am. Chem. Soc.* **2004**, *126*, 13255–13264.

(12) (a) Hennig, A.; Matile, S. *Chirality* **2008**, *20*, 932–937. (b) Ma, L.; Melegari, M.; Colombini, M.; Davis, J. T. *J. Am. Chem. Soc.* **2008**, *130*, 2938–2939. (c) Lee, M. P. H.; Parkinson, G. N.; Hazel, P.; Neidle, S. *J. Am. Chem. Soc.* **2007**, *129*, 10106–10107. (d) Kaucher, M. S.; Harrell, W. A.; Davis, J. T. *J. Am. Chem. Soc.* **2006**, *128*, 38–39. (e) Sakai, N.; Kamikawa, Y.; Nishii, M.; Matsuoka, T.; Kato, T.; Matile, S. *J. Am. Chem. Soc.* **2006**, *128*, 2218–2219. (f) Forman, S. L.; Fettinger, J. C.; Pieraccini, S.; Gottareli, G.; Davis, J. T. *J. Am. Chem. Soc.* **2000**, *122*, 4060–4067.

(13) (a) Huang, C. C.; Chang, H. T. *Chem. Commun.* **2008**, 1461–1463. (b) He, F.; Tang, Y. L.; Yu, M. H.; Feng, F.; An, L. L.; Sun, H.; Wang, S.; Li, Y. L.; Zhu, D. B.; Bazan, G. C. *J. Am. Chem. Soc.* **2006**, *128*, 6764–6765. (c) He, F.; Tang, Y. L.; Wang, S.; Li, Y. L.; Zhu, D. B. *J. Am. Chem. Soc.* **2005**, *127*, 12343–12346. (d) Ueyama, H.; Takagi, M.; Takenaka, S. *J. Am. Chem. Soc.* **2002**, *124*, 14286–14287.

(14) Phan, A. T.; Mergny, J. L. *Nucleic Acids Res.* **2002**, *30*, 4618–4625.

(15) Sen, D.; Gilbert, W. *Nature* **1990**, *344*, 410–414.

(16) (a) Wharton, J. E.; Jin, P.; Sexton, L. T.; Horne, L. P.; Sherrill, S. A.; Mino, W. K.; Martin, C. R. *Small* **2007**, *3*, 1424–1430. (b) Harrell, C. C.; Siwy, Z. S.; Martin, C. R. *Small* **2006**, *2*, 194–198. (c) Siwy, Z.; Apel, P.; Baur, D.; Dobrev, D. D.; Korchev, Y. E.; Neumann, R.; Spohr, R.; Trautmann, C.; Voss, K. O. *Surf. Sci.* **2003**, *532*, 1061–1066. (d) Apel, P. Y.; Korchev, Y. E.; Siwy, Z.; Spohr, R.; Yoshida, M. *Nucl. Instrum. Meth. B* **2001**, *184*, 337–346.
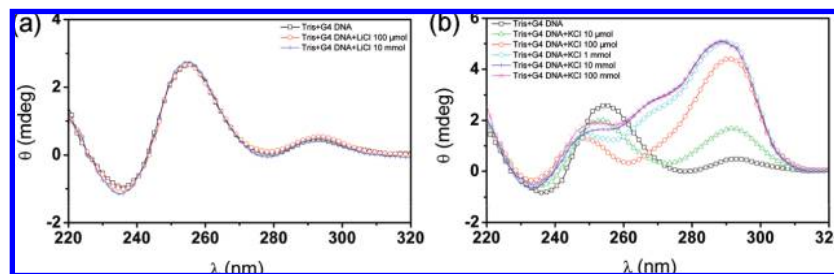
Scheme 1[a]

[a] G4 DNA was immobilized onto the inner surface of a single nanopore. (a) There is no K^+; the G4 DNA relaxes to a loosely packed single-stranded structure. (b) Presence of K^+; the G4 DNA folds into densely packed rigid quadruplex structures that partially decrease the effective pore size of the nanopore. (c) After adding complementary DNA strands, G4 DNA forms a closely packed arrangement of double-stranded DNA on the single nanopore. The fluorescent group Bodipy493/503 (green circle) located at 3′-end of the attached DNA molecule. Before modification, the etched funnel-shaped single nanopores are around 20 nm wide at the narrowest point (drawing not to scale).

K^+ increased from 0 to 10 mM, G4 DNA showed a positive peak near 290 nm, a crossover at around 260 nm, and weak negative peaks near 255 and 235 nm, thereby indicating a typical G4 conformation.[11b,17] According to the positive peak near 290 nm, when the concentration of K^+ increased up to 100 mM, the CD signal did not change significantly. It indicated that the major structure of this DNA was G4 conformation within the concentration range from 0 to 10 mM. Considering that the BNCS was realized by folding and unfolding of the G4 DNA, K^+ concentration range was determined by G4 conformational change. Thus, this K^+ concentration range was considered as the maximum range for the BNCS current measurements.

In addition, owing to the molecules of fluorin contained in the fluorescent group Bodipy493/503 (green circle, Scheme 1) at the 3′-end of the attached DNA molecule, DNA-modified surface of the PET films was also determined by the contact angle measurements and the X-ray photoelectron spectroscopy analysis (see Supporting Information, Figure S1 and Tables S1−S3).

Ion transport properties of the nanopore were examined by current measurements. Some previous studies related to PET nanopores have shown that there were two major influencing

factors bringing the change of measuring current at the same voltage: ion concentration of the electrolyte solution[16b,18] and the effective pore size of the nanopore.[6] It was assumed that the effective pore size of the nanopore was determined by two aspects in this BNCS, that is, the change of physical block and charge density by the biomolecular conformational change. In our strategies, the physical block and charge density would change simultaneously because the responsive DNA molecules were highly negatively charged in the pH-neutral environment. In the following experiments, these two factors were integrated to investigate the "effective pore size" change, which could more comprehensively explain the new phenomenon in this BNCS. According to the fact that the nanopore wall[7,19] before and after G4 DNA modification is negatively charged under the neutral conditions, the electrolyte solutions in all of the experiments were buffered to a pH value of 7.2 using 5 mM Tris-HCl at 23 °C in order to avoid the influence from pH.

Figure 2a shows a positive correlation between Li^+ concentration and the current before G4 DNA modification, which means that the current increased with Li^+ concentration from 0 to 1500 μM at 2 V (anode facing the tip of the nanopore). After modification, the currents also show a similar increasing trend, but they were lower than that before modification at the same concentration, which could be attributed to the covalently attached DNA molecules that induced a relative reduction of the effective pore size.[4] Whereas the hybridization of the complementary DNA strands with G4 DNA resulted in a sharp decrease in the currents, it still kept an increasing trend.

Figure 2b shows the current change of the nanopore via the concentration at different states upon the addition of K^+. Before G4 DNA modification and after the hybridization, the currents indicated an increasing trend similar to that in Figure 2a. It is worth specially mentioning that there was a remarkable difference after DNA modification. The currents first started to drop with K^+ concentration increasing from 0 to 500 μM, and then the currents changed a little at the concentration range from 500 to 750 μM. Afterward, the concentration further increased from 750 to 1500 μM, and the currents showed an increasing trend again. This unusual phenomenon could be attributed to the formation of G4 structures that induced the relatively dense packing of DNA molecules on the inner wall of the nanopore, resulting in an efficient decrease of the effective pore size and thus the current change. These results coincided with our previous studies on the four-stranded i-motif structure.[6] Before the formation of G4 structures, G4 DNA with the single-stranded structure loosely packing on the nanopore wall could not efficiently reduce the effective pore size, leading to the currents increasing with Li^+ concentration changing from 0 to 1500 μM (Figure 2a). However, the hybridization of the complementary DNA strands with G4 DNA formed the rigid duplex structure of DNA and thus created a closely packed arrangement of double-stranded DNA structure that was more stable than the G4 structure (Scheme 1c). Therefore, G4 DNA conformation could not change with K^+ concentration increasing. This deduction was strongly supported by further experimental data from the CD method.

As shown in Figure 3, after adding the complementary DNA strands, the rigid duplex structures of DNA formed. No change could be observed when K^+ concentration changed from 0 to 1500 μM, which meant the double-stranded DNA conformation was more stable than that at other states.

(17) Xu, Y.; Noguchi, Y.; Sugiyama, H. *Bioorg. Med. Chem.* **2006**, *14*, 5584–5591.

(18) (a) Powell, M. R.; Sullivan, M.; Vlassiouk, I.; Constantin, D.; Sudre, O.; Martens, C. C.; Eisenberg, R. S.; Siwy, Z. S. *Nat. Nanotechnol.* **2008**, *3*, 51–57. (b) Siwy, Z. S. *Adv. Funct. Mater.* **2006**, *16*, 735–746. (c) Siwy, Z.; Kosinska, I. D.; Fulinski, A.; Martin, C. R. *Phys. Rev. Lett.* **2005**, *94*, 048102. (d) Schiedt, B.; Healy, K.; Morrison, A. P.; Neumann, R.; Siwy, Z. *Nucl. Instrum. Meth. B* **2005**, *236*, 109–116. (e) Kumar, S.; Kumar, S.; Chakarvarti, S. K. *Radiat. Meas.* **2003**, *36*, 757–760. (f) Siwy, Z.; Apel, P.; Dobrev, D.; Neumann, R.; Spohr, R.; Trautmann, C.; Voss, K. *Nucl. Instrum. Meth. B* **2003**, *208*, 143–148. (g) Siwy, Z.; Fulinski, A. *Phys. Rev. Lett.* **2002**, *89*, 198103.

(19) Siwy, Z.; Heins, E.; Harrell, C. C.; Kohli, P.; Martin, C. R. *J. Am. Chem. Soc.* **2004**, *126*, 10850–10851.

Figure 1. CD spectra of G4 DNA (5′-GGG TTA GGG TTA GGG TTA GGG-3′) conformations in the different concentration of alkali metal ions. (a) Concentration of Li$^+$ of 0 μM ($\square$, black), 100 μM ($\bigcirc$, red), 10 mM (+, blue). (b) Concentration of K$^+$ of 0 μM ($\square$, black), 10 μM ($\triangle$, green), 100 μM ($\bigcirc$, red), 1 mM ($\diamond$, cyan), 10 mM (+, blue), 100 mM ($\times$, magenta) in Tris-HCl (5 mM, pH 7.2 at 23 °C).
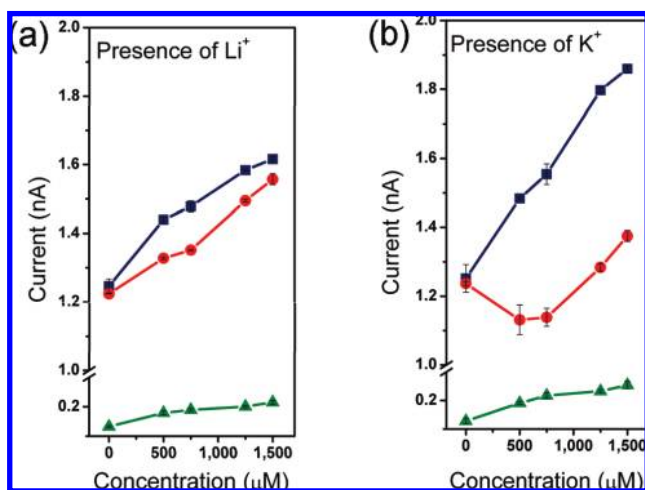

Figure 2. Current−concentration (I−C) properties of a single nanopore embedded in a PET membrane before and after G4 DNA molecules attached onto the pore wall in Tris-HCl (5 mM, pH = 7.2, at 23 °C). (a) Presence of different Li$^+$ concentration. (b) Presence of different K$^+$ concentration. Before G4 DNA modification ($\blacksquare$, blue); after G4 DNA modification ($\bullet$, red); after the addition of the complementary DNA strands (5′-CCC TAA CCC TAA CCC TAA CCC-3′) ($\blacktriangle$, green). Before modification, the diameters of the tip and base are about 18 and 420 nm, respectively.
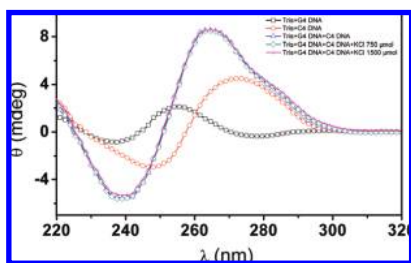
Figure 3. CD spectra of G4 DNA (5′-GGG TTA GGG TTA GGG TTA GGG-3′), the complementary DNA strands (5′-CCC TAA CCC TAA CCC TAA CCC-3′), and double-stranded DNA (G4 DNA and the complementary DNA strands). G4 DNA in Tris-HCl ($\square$, black); the complementary DNA strands in Tris-HCl ($\bigcirc$, red); double-stranded DNA in the different concentration of K$^+$ ions (0 μM, $\triangle$, blue; 750 μM, $\diamond$, green; 1500 μM, +, magenta).

To exclude the possible effect of regular DNA of which conformation was not responsive to K$^+$, poly-A DNA[6] was selected in this study. From Figure 4, when the system was at its initial state without the alkali metal ions, poly-A DNA showed a negative peak near 247 nm.[6] No change could be observed when the concentration of both K$^+$ and Li$^+$ of the buffer solution changed from 0 to 10 mM (G4 conformation appeared at the same K$^+$ concentration), which indicated there

was no distinct conformational change, strongly suggesting that the conformation of poly-A DNA was not responsive to K$^+$ or Li$^+$.

Figure 5 shows the current change of a conical nanopore upon the addition of Li$^+$ or K$^+$ before and after poly-A DNA modification under the same conditions, respectively. The ion transport properties of the nanopore at different states also showed the increasing trend. It was reasonable that poly-A DNA with single-stranded structure loosely packing on the pore wall could not efficiently reduce the effective pore size, leading to the currents increasing at the ion concentration ranging from 0 to 1500 μM. These results again verified that the new phenomenon of the current change for K$^+$ after G4 DNA modification was mainly due to the conformation change of G4 DNA.

In this work, the diameter of the tip around 20 nm was selected to study this BNCS as the optimized pore size discussed in the previous work.[6] As shown in Figure 6, all of the nanopores before modification, whose tip diameters range from 17 to 24 nm, had ratios higher than 1 and exhibited the synthetic nanopore original property that the current measurements had a positive correlation with alkali metal ion concentration. After the nanopores were modified with G4 DNA, their ratios showed the same trend for Li$^+$, but they were totally different for K$^+$, in which the ratios were less than 1. Compared to the original nanopore, the nanopores modified with poly-A DNA showed similar increasing trend for both Li$^+$ and K$^+$. Therefore, the conformational change exhibited in G4 DNA molecules indeed contributes to this new phenomenon in the BNCS.

To explore this phenomenon observed from Figure 2b that the currents first decreased and then increased with changing K$^+$ concentration, the CD melting method was utilized.[11a,c] It is well-known that G4 DNA melting reveals the ratio of folding and unfolding of G4 DNA and corresponds to the stability of the G4 structures.[11c] Figure 7 indicates that the stability of the G4 structures increased with K$^+$ concentration increasing. The cyan horizontal dotted line represents the temperature (T_{et}) for the current measurement. When K$^+$ concentration exceeded C_{et} (the corresponding concentration of the intersection point between the black curve and the cyan horizontal dotted line), the G4 structures became more and more stable with increasing K$^+$ concentration. With the stability of structures further enhancing, however, the change of the DNA melting rate showed a type of "L" curve (Figure 7, insets), which means that, for this kind of G4 DNA, K$^+$ concentration reached a certain level, and the stability of the G4 structures was nearly kept unchanged. It is found that the most prominent stabilizing of the G4 DNA structure occurred below a K$^+$ concentration of 750 μM.

On the basis of the above analyses, it can be concluded that the enhanced stability of the G4 structures by increasing
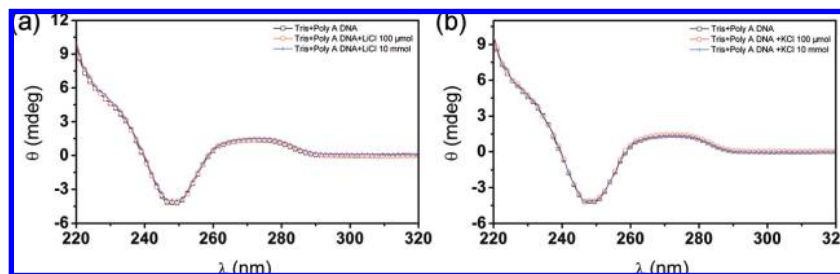
Figure 4. CD spectra of poly-A DNA (5′-AA AAA AAA AAA AAA AAA AAA-3′) conformations in the different concentration of alkali metal ions. (a) Li⁺, (b) K⁺; 0 μM (□, black), 100 μM (○, red), 10 mM (+, blue) in Tris-HCl (5 mM, pH 7.2 at 23 °C).
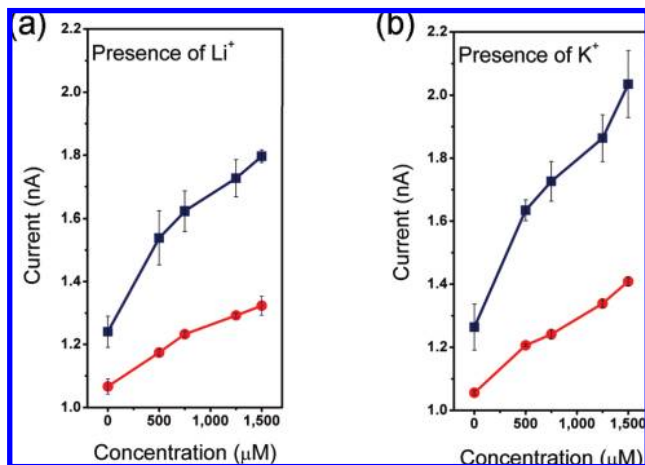

Figure 5. *I−C* properties of a single nanopore before and after poly-A DNA molecules attached onto the inner pore wall. (a) Li⁺, (b) K⁺. Before modification (■, blue); after modification (●, red). Before modification, the diameters of the tip and base are about 17 and 400 nm, respectively.

Figure 7. DNA melting−ion concentration curve of G4 DNA (5′-GGG TTA GGG TTA GGG TTA GGG-3′). The insets represent the stability of G4 structure under different K⁺ concentration at the fixed experimental temperature and influence of different K⁺ concentration on the slope of G4 DNA melting and K⁺ concentration.

increased stability of G4 structures gradually decreased, the ion concentration started to exert a main influence.

Conclusions

In summary, we experimentally demonstrate a novel biomimetic nanochannel which can achieve a K⁺ response within a certain ion concentration range. The situation of the grafting G4 DNA on a single nanopore can closely imitate the in vivo condition[11c] because the G-rich telomere overhang is attached to the chromosome. Therefore, this artificial system could promote a potential to conveniently study biomolecule conformational change in confined space by the current measurement which is significantly different from the nanopore sequencing.[20] Moreover, such a system as a basic platform could potentially spark further experimental and theoretical efforts to simulate the process of ion transport in living organisms and boost the
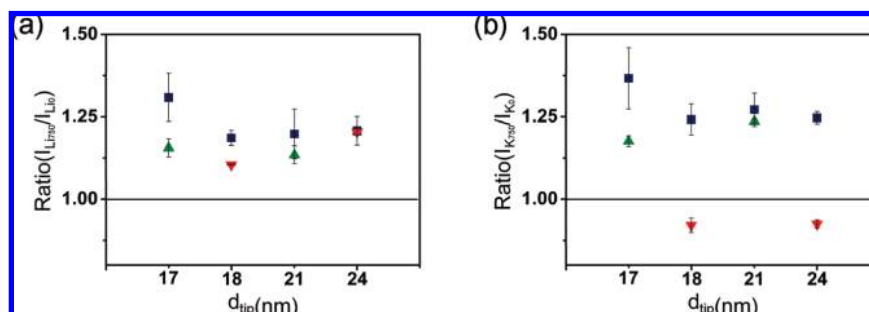
K⁺ concentration could gradually decrease the effective pore size of the nanopore within a certain ion concentration range from 0 to 750 μM. On the other aspect, K⁺ concentration exhibited a positive correlation with the current change (Figure 2b). Therefore, this new phenomenon of the ion transport properties of the nanopore modified with G4 DNA was explained by the competition between these two factors, that is, the stability of G4 structures and ion concentration. To be clearer, when the stability of G4 structures highly increased with increasing K⁺ concentration, it played a prominent role in ion transport properties of the nanopore by adjusting the effective pore size, whereas when the

Figure 6. Current ratio of the nanopores under the absence and presence of 750 μM alkali metal ions before and after DNA modification. (a) Li⁺, (b), K⁺. Before modification (■, blue), after G4 DNA modification (▼, red), after poly-A DNA modification (▲, green). The diameters of the tip and base are about 20 and 400 nm (sample 1, ~17 and ~ 400 nm; sample 2, ~18 and 420 nm; sample 3, ~21 and ~400 nm; sample 4, ~24 and ~410 nm).

development of bioinspired intelligent nanopore apparatus such as biosensors,[21] molecular filtration,[22] and nanofluidic devices.[23]

Experimental Section

CD Spectroscopy Measurements. CD spectra were collected on a JASCO J-810 CD spectrometer. CD spectra were measured at 23 °C, as maintained by the temperature-control units affiliated with the spectrometers. Wavelength scans were performed between 220 and 320 nm. Quartz cells with a path length of 1 mm were used for DNA and Tris solutions. The DNA was dissolved in a Tris buffer solution (pH = 7.2) containing Tris (5 mM) and HCl (4.5 mM) to give the DNA-Tris buffer solution a final concentration of 1 μM in a quartz cell. CD-melting profile was recorded at 290 nm. The temperature increased from 10 to 90 °C. The average heating rate was about 1 °C/min.

Nanopore Preparation. The single conical nanopore was produced in polymer films using the well-developed ion track-etching technique (see Supporting Information, Scheme S1). In this work, the base diameter was usually several hundred nanometers and the tip diameter was around 20 nm.

DNA Immobilization. The amino single-stranded G4 DNA (5′-(NH$_2$)-(CH$_2$)$_6$-AAA AAA AAA AGG GTT AGG GTT AGG GTT AGG G (Bodipy493/503)-3′) on the 5′-end and poly-A DNA(5′-(NH$_2$)-(CH$_2$)$_6$-AAA AAA AAA AAA AAA AAA AAA AAA AAA AAA A (Bodipy493/503)-3′) on the 5′-end were immobilized onto the PET surface and inner pore wall by a two-step chemical reaction, as illustrated in Scheme S2. The NHSS ester was formed by exposure of the single-pore-contained PET film to an aqueous solution (1 mL of Milli-Q water, 18.2 MΩ) of 15 mg of EDC and 3 mg of NHSS for 1 h at 23 °C. These PET-NHSS ester monolayers were reacted for 2 h with a solution of 1 μM amino DNA in Milli-Q water at 23 °C. Then, the PET film had been stored for 1 day in Tris buffer (pH = 7.2, 23 °C) containing Tris (5 mM) and HCl (4.5 mM) before further experiments. The chemical covalent modification in this system is irreversible.

Current Measurement. The nanopore conductivity and the ion responsive properties of the DNA molecules were studied by measuring ion current through the unmodified nanopores or DNA-modified nanopores. Ion current was measured by a Keithley 6487 picoammeter (Keithley Instruments, Cleveland, OH). A single-pore PET membrane was mounted between two chambers of the etching cell mentioned above (Scheme S3). Ag/AgCl electrodes were used to apply a transmembrane potential across the film. Forward voltage was the potential applied on the base side (Scheme S1). The main transmembrane potential used in this work was a scanning voltage varied from −2 to +2 V with a 40 s period (Figures S2 and S3). Current measurement was conducted on the sample treated with Tris solution containing different concentration of alkali metal ions for 1 h before data collection at 23 °C. Each test was repeated five times to obtain the average current value at different voltage.

Supporting Information Available: Synthetic procedures, contact angle measurements, XPS test, current−voltage properties of the single nanopore before and after DNA molecules attachment onto the inner pore wall, thermal melting profiles of G4 DNA, and the complete ref 20. This material is available free of charge via the Internet at http://pubs.acs.org.

JA901574C

(20) Branton, D.; et al. *Nat. Biotechnol.* **2008**, *26*, 1146–1153.
(21) (a) Martin, C. R.; Siwy, Z. S. *Science* **2007**, *317*, 331–332. (b) Choi, Y.; Baker, L. A.; Hillebrenner, H.; Martin, C. R. *Phys. Chem. Chem. Phys.* **2006**, *8*, 4976–4988.
(22) Jirage, K. B.; Hulteen, J. C.; Martin, C. R. *Science* **1997**, *278*, 655–658.
(23) Huh, D.; Mills, K. L.; Zhu, X. Y.; Burns, M. A.; Thouless, M. D.; Takayama, S. *Nat. Mater.* **2007**, *6*, 424–428.